JOURNAL OF VIROLOGY, May 2002, p. 4559–4566 Vol. 76, No. 9
0022-538X/02/$04.00+0 DOI: 10.1128/JVI.76.9.4559–4566.2002

Adeno-Associated Virus Capsids Displaying Immunoglobulin-Binding Domains Permit Antibody-Mediated Vector Retargeting to Specific Cell Surface Receptors

Martin U. Ried,[1] Anne Girod,[1] Kristin Leike,[1] Hildegard Büning,[1] and Michael Hallek[1,2,3]*

Laboratorium für Molekulare Biologie, Genzentrum,[1] and Medizinische Klinik III, Klinikum Grosshadern,[2] Ludwig-Maximilians-Universitaet Muenchen, and GSF-National Center for Research and Environment, KKG Gentherapie,[3] 81377 Munich, Germany

Received 10 September 2001/Accepted 18 January 2002

Recombinant adeno-associated virus type 2 (rAAV2) is a promising vector for human somatic gene therapy. However, its broad host range is a disadvantage for some applications, because it reduces the specificity of the gene transfer. To overcome this limitation, we sought to create a versatile rAAV vector targeting system which would allow us to redirect rAAV binding to specific cell surface receptors by simple coupling of different ligands to its capsid. For this purpose, an immunoglobulin G (IgG) binding domain of protein A, Z34C, was inserted into the AAV2 capsid at amino acid position 587. The resulting AAV2-Z34C mutants could be packaged and purified to high titers and bound to IgG molecules. rAAV2-Z34C vectors coupled to antibodies against CD29 (β_1-integrin), CD117 (c-kit receptor), and CXCR4 specifically transduced distinct human hematopoietic cell lines. In marked contrast, no transduction was seen in the absence of antibodies or in the presence of specific blocking reagents. These results demonstrate for the first time that an immunoglobulin binding domain can be inserted into the AAV2 capsid and coupled to various antibodies, which mediate the retargeting of rAAV vectors to specific cell surface receptors.

The human parvovirus adeno-associated virus type 2 (AAV2) has many features that make it attractive as a vector for human somatic gene therapy (9, 11). However, its broad host range might represent a limitation for some applications, because recombinant AAV (rAAV)-mediated gene transfer would not be specific for the tissue or cell type of interest. The host range is determined by the interaction of the AAV2 capsid with specific cellular receptors and coreceptors (18, 26, 27).

Recently, a hypothetical model of the AAV capsid was generated, and several regions which were exposed on the viral capsid accepted the insertion of an integrin-specific 14-amino-acid (aa) RGD ligand (L14) and bound to target cells expressing the corresponding receptor (6). Moreover, AAV2 vectors with a ligand insertion at site 587 infected wild-type AAV-resistant B16F10 melanoma cells with infectious targeting titers of 5×10^4 LacZ expression-forming units (EFU) per ml (multiplicity of infection, 1), indicating that the susceptibility of these cells to AAV2 infection was increased by at least 4 orders of magnitude (6).

However, with this approach it remained difficult and laborious to generate targeting vectors, because the design and optimization of new AAV capsid mutants were required for each specific receptor and cell type. Thus, it seemed desirable to generate a universal AAV targeting capsid on which different ligands could bind and redirect the virus to specific cell surface receptors (Fig. 1A). Such a vector would allow rapid screening of appropriate receptors mediating virus binding, uptake, and correct intracellular processing, which are all prerequisites for successful retargeting of AAV-based vectors.

For this purpose, an immunoglobulin G (IgG) binding domain was introduced into the capsid to enable AAV to bind different antibodies via their Fc regions. In these virus-antibody conjugates, the variable domain of the respective antibodies would function as a ligand directed against a specific cell surface receptor. A similar strategy has already been used for the retargeting of Sindbis virus vectors (15, 16). The IgG binding molecule chosen for our experiments was a minimized and optimized domain of protein A from *Staphylococcus aureu*s, Z34C (25). Z34C is a 34-aa two-helix domain which shows only a twofold-reduced binding affinity in comparison to the natural B domain.

By use of Z34C insertion mutants, rAAV was retargeted to hematopoietic cell lines which were poorly transduced by rAAV carrying the wild-type capsid (10, 17) via a specific interaction with the cell surface receptor CD29 (β_1-integrin), CD117 (c-kit), or CXCR4 (13, 32).

MATERIALS AND METHODS

Plasmids. Plasmid pUC-AV2 was constructed by subcloning the 4.8-kb *Bgl*II fragment of pAV2 (12) (ATCC 37216) into the *Bam*HI site of pUC19 (New England Biolabs) by blunt-end ligation. It contained the full-length AAV2 genome and served as the parental plasmid for all constructs described in this report.

Plasmid pCap was obtained by blunt-end subcloning of the 2.2-kb *Eco*RI-*Bsp*MI fragment of pUC-AV2 into the *Eco*RI site of pUC19; therefore, it contained only the *cap* gene. It served as a template for all PCRs.

The mutated plasmids contained the full-length AAV2 genome; the Z34C-encoding sequence was inserted in the *cap* gene of the AAV2 genome after the sequence for amino acid 587 (p587Z34C) or in combination with a deletion of amino acids 581 to 589 after the sequence for amino acid 580 (p587Δ9Z34C). Mutagenesis was achieved by using an ExSite PCR-based site-directed mutagenesis kit as described by the supplier (Stratagene). For the two mutants, a PCR

* Corresponding author. Mailing address: Genzentrum, Universitaet Muenchen, Feodor-Lynen-Str. 25, D-81377 Munich, Germany. Phone: 49-89-2180-6774. Fax: 49-89-2180-6797. E-mail: mhallek@med3.med.uni-muenchen.de.

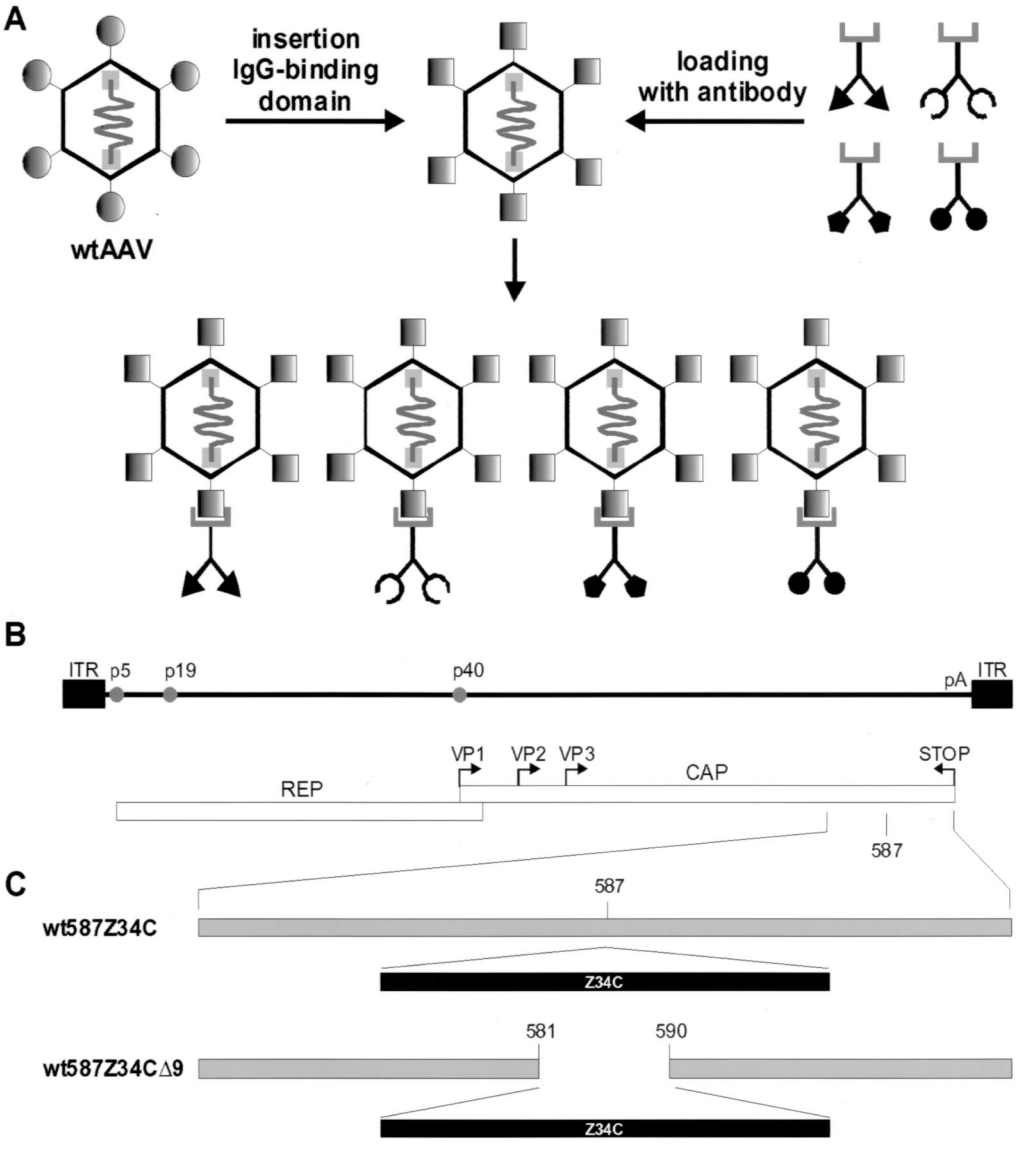

FIG. 1. (A) Strategy for retargeting AAV2 vectors with immunoglobulin-binding domains. The wild-type AAV2 (wtAAV) capsid is modified by insertion of the Z34C immunoglobulin binding domain. The mutated virus capsid is loaded with targeting antibodies against specific cell surface receptors. (B) Genomic structure of wild-type AAV2. The positions of the p5, p19, and p40 viral promoters and the polyadenylation signal (pA) are indicated. Symbols show ITRs, *rep* and *cap* coding regions, and initiation and stop codons for the VP1, VP2, and VP3 viral capsid proteins. (C) Schematic diagram of the generated Z34C capsid mutants. The insertion site at position 587, the deleted amino acids (positions 581 to 589), and the Z34C ligand are indicated.

fragment was generated by using plasmid pCap as the template and two primers: one (FOR) containing nucleotides belonging to the *cap* gene immediately upstream of the insertion site and some nucleotides coding for the 5′ portion of the Z34C ligand and the other (BACK) containing nucleotides belonging to the *cap* gene immediately downstream of the insertion site and some nucleotides coding for the 3′ portion of the Z34C peptide.

The following primers were used: 580Z34C-BACK (5′-ATTAGGATCGTGGAGGGCTTCGTAAAAGCGTGCGTTGACATTGCATATTAAAAGATACAGAACCATA-3′), 587Z34C-BACK (5′-ATTAGGATCGTGGAGGGCTTCGTAAAAGCGGCGTTGACATTGCATATTAAAGTTGCCTCTCTGGAG-3′), 587Z34C-FOR (5′-TTAAATGAAGAACAACGCAATGCCAAGATTAAGAGTATTCGCGATGATTGTAGACAAGCAGCTACC-3′), and 590Z34C-FOR (5′-TTAAATGAAGAACAACGCAATGCCAAGATTAAGAGTATTCGCGATGATTGTGCACTCCGCAGAT-3′).

The PCR products were amplified in bacteria and sequenced. The 1.4-kb *Eco*NI-*Xcm*I fragment containing the Z34-encoding sequence was then subcloned into pUC-AV2 from which the corresponding fragment encoding the wild-type *cap* sequence had been removed.

Plasmid pRC was constructed by blunt-end subcloning of the 4.5-kb *Xba*I-*Xba*I fragment of psub201(+) (22) (plasmid obtained from R. J. Samulski) into the *Pst*I-*Bam*HI sites of pSV40oriAAV (3).

Plasmids pRC587Z34C and pRC587Δ9Z34C were derived from plasmid pRC by subcloning of the *Eco*NI-*Xcm*I fragments of p587Z34C and p587Δ9Z34C into pRC from which the corresponding fragment had been removed. The plasmids contained the AAV2 *rep* and *cap* coding regions but lacked the viral inverted terminal repeats (ITRs); therefore, they allowed the production of helper-free AAV2-based vectors either with a wild-type AAV2 capsid (pRC) or with a capsid presenting the Z34C peptide.

Plasmid pGFP is an AAV2-based vector plasmid in which the AAV2 ITR sequences flank the hygromycin selectable marker gene controlled by the thy-

midine kinase promoter and the *Aequorea victoria* green fluorescence protein (GFP) gene promoted by the cytomegalovirus promoter. pGFP was generated by inserting the *Asp*718-*Not*I fragment of pEGFP-N1 (Clontech) into the *Asp*718-*Not*I sites of psub/CEP4(Sal inverse). psub/CEP4(Sal inverse) was a derivative of psub201(+) (22) that had been digested with *Xba*I, blunt ended, and ligated to a blunt-ended 3,923-bp *Sal*I-*Nru*I fragment of pCEP4(Sal inverse). pCEP4(Sal inverse) differs from pCEP4 (Invitrogen) by inversion of the *Sal*I-*Sal*I fragment from positions 8 to 1316.

Cell cultures. Cell lines HeLa (ATCC CCL-2), 293 (ATCC CRL-1573), and Jurkat (ATCC CRL-1990) were provided by the American Type Culture Collection. M-07e and Mec1 cells were described previously (1, 24) and were obtained from J. Griffin (Boston) and F. Caligaris-Cappio (Turin), respectively. They were maintained at 37°C in 5% CO_2 as monolayer cultures in Dulbecco's modified Eagle's medium (HeLa and 293) or as suspension cultures in RPMI 1640 medium (Jurkat, M-07e, and Mec1). The medium was supplemented with 10% fetal calf serum, 100 U of penicillin/ml, 100 μg of streptomycin/ml, 2 mM L-glutamine, and 10 ng of interleukin 3/ml (M-07e).

Production of AAV2 particles. 293 cells were seeded in 20 culture dishes (150-mm diameter, each containing 7.5×10^6 293 cells) and cotransfected by the calcium phosphate method with a total of 37.5 μg of vector plasmid (pGFP), packaging plasmid pRC, and adenovirus plasmid pXX6-80 (obtained from J. Samulski) at a 1:1:1 molar ratio. For viruses containing AAV *rep* and *cap* genes, plasmid pUC-AV2 or a mutated plasmid was transfected with pXX6-80 at a 1:1 molar ratio. After 24 h, the transfection medium was replaced with fresh Dulbecco's modified Eagle's medium containing 2% fetal calf serum, and the cells were incubated for 24 h at 37°C in 5% CO_2. Thereafter, cells were harvested and pelleted by low-speed centrifugation at $3,000 \times g$. Cells were resuspended in 150 mM NaCl–50 mM Tris-HCl (pH 8.5)–1 mM $MgCl_2$ and sonicated. Cell debris was spun down at $3,700 \times g$ for 20 min at 4°C. The supernatant was purified by ammonium sulfate precipitation. Contaminants were precipitated with 35% ammonium sulfate. After centrifugation, the viral particles in the supernatant were precipitated in 55% ammonium sulfate. The pellet was resuspended in PBS-MK buffer (phosphate-buffered saline [PBS], 1 mM $MgCl_2$, 2.5 mM KCl) and loaded onto an iodixanol gradient (4, 31, 34). Briefly, the solution containing the resuspended virus was transferred into an Optiseal centrifuge tube (26 × 77 mm; Beckman) by layering in the following order: 7 ml of 15% iodixanol and 1 M NaCl in PBS-MK buffer, 5 ml of 25% iodixanol in PBS-MK buffer, 5 ml of 40% iodixanol in PBS-MK buffer and, finally, 6 ml of 60% iodixanol in PBS-MK buffer. All the iodixanol buffers, with the exception of the 40% buffer, contained phenol red. The tube was centrifuged in a type 70 Ti rotor (Beckman) at 69,000 rpm for 1 h at 18°C. The 40% iodixanol phase containing the virus was collected and dialyzed against PBS-MK buffer.

Titer determinations. The concentration of DNA containing viral particles was determined by DNA dot blot hybridization. AAV2 preparations were first incubated with 500 μg of DNase I/ml to remove DNA including putatively free viral genomes that could be subsequently hybridized with the probe. The viral preparations were then blotted in serial dilutions and finally hybridized with a random-primer *rep* or *gfp* probe by standard methods. Particle titers were determined by comparing the intensity of the hybridization signal with that obtained for a plasmid standard of a known concentration blotted on the same membrane.

The titer was also tested by an enzyme-linked immunosorbent assay (ELISA) with murine monoclonal antibody (MAb) A20, which recognizes only assembled capsids of AAV2 (7, 28). Purified MAb A20 (200 ng) was attached to Costar microtiter plates by overnight incubation at 4°C. After blocking with PBS containing 10% bovine serum albumin (BSA) and 0.05% Tween 20, serial dilutions of AAV2 preparations were added to the wells and incubated for 3 h at room temperature. After a wash with PBS, the wells were incubated with biotin-conjugated MAb A20 for 1 h at room temperature. After a second wash, the wells were incubated with peroxidase-conjugated streptavidin (Dianova) for 1 h at room temperature. After a wash, 100 μl of substrate solution (0.1 M sodium citrate buffer [pH 6.0] containing 0.1 μg of 3,3′,5,5′-tetramethylbenzidine and 0.003% H_2O_2) was added to each well. After 10 min, the reaction was stopped with 50 μl of 1 M H_2SO_4, and the light absorbance at 450 nm was measured with an automated microplate reader (MWG). Particle titers were determined by comparing the absorbance with that obtained for a viral preparation of a known titer (measured by electron microscopy) added to the same plate.

Electron microscopy. Electron microscopy was done at DKFZ, Heidelberg, Germany. Iodixanol gradient-purified and PBS-MK-dialyzed viral particles were adsorbed onto Formvar-carbon-coated copper grids and negatively stained with uranyl acetate. Empty capsids could be recognized as black viral particles, and full capsids were recognized as bright particles. Titers were calculated in comparison to a known viral standard.

TABLE 1. Capsid formation and natural tropism of the AAV2-Z34 capsid mutant virions

Virus	No. of genomic particles/ml	Infectious titer on HeLa cells[a]	No. of particles/ml	
			$A20^+$ epitope[b]	EM capsid[c]
wtAAV2[d]	5×10^{13}	5×10^9	1×10^{12}	6×10^{13}
wt587Z34C[d]	2×10^{12}	3×10^5	1×10^{10}	3×10^{12}
wt587Δ9Z34C[d]	5×10^{13}	1×10^6	1×10^{11}	7×10^{13}
rAAV-GFP[e]	1×10^{12}	5×10^7	ND	ND
rAAV-GFP587Z34C[e]	5×10^{10}	2×10^4	ND	ND
rAAV-GFP587Δ9Z34C[e]	5×10^{10}	2×10^4	ND	ND

[a] Expressed as Rep EFU/ml for preparations with the viral *rep* gene or as GFP EFU/ml for preparations with the GFP transgene.
[b] Detection of A20-positive ($A20^+$) epitopes by an ELISA. ND, not done.
[c] Detection of capsid particles by electron microscopy (EM).
[d] Containing the wild-type AAV2 genome.
[e] Containing the GFP transgene.

IgG binding ELISA. The surface expression and functionality of the Z34C ligand on viral capsids was measured by an IgG binding ELISA. Serial dilutions of viral preparations were used to coat 96-well plates (Costar) overnight at 4°C and were blocked with PBS containing 2% BSA and 0.05% Tween. After a wash with PBS, biotinylated rabbit antibody (Dianova) was added (2.5 μg/ml in PBS, 100 μl/well), and the plates were incubated at room temperature for 1 h. Detection of Z34C-bound biotinylated antibody was performed as described above.

Infection assays and infectious titer determinations. For retargeting infection assays, 2×10^5 cells were seeded in 48-well plates and irradiated with 70 Gy from a ^{137}Cs gamma irradiation source (GSF, Grosshadern, Germany). Genomic viral particles (5×10^8) were incubated with 1 μg of targeting antibody, protein A (final concentration, 10 μg/ml), rabbit IgG (final concentration, 2 μg/ml), or heparin (final concentration, 100 μg/ml) for 30 min at room temperature. Cells were incubated with virus solution in 300 μl of serum-free medium for 60 min at 37°C in 5% CO_2 and then supplemented with 35 μl of serum. After 24 h, the infection solution was replaced with 1 ml of serum-containing medium. Titers were determined 48 h after infection by counting infected cells by fluorescence microscopy. The optimum of 1 μg of targeting antibody was determined in separate dilution experiments (data not shown). Infectious titers of virus stocks with the wild-type gene (Rep EFU) were determined by in situ detection of Rep protein synthesis in an immunofluorescence assay with anti-Rep antibody or by microscopic detection of virus containing a GFP transgene as described before (6, 8).

All transduction experiments were carried out at least three times.

RESULTS

Generation of AAV2-Z34C mutants. To retarget AAV2, the minimized Z34C protein A binding domain (25) was inserted into the *cap* gene at site 587. Site 587 was shown to accept the insertion of a targeting ligand, to express this ligand at the capsid surface, and to allow retargeting of AAV2 or rAAV vectors (6). The minimized Z34C domain was chosen because the size of the insertion at site 587 was limited to approximately 30 aa (unpublished data). One insertion at site 587 and one insertion in combination with a deletion of 9 aa were used in order to reduce the length of the loop predicted at this position by a hypothetical AAV surface model (6) (Fig. 1C).

AAV2-Z34C mutants package the viral genome, express Z34C at the capsid surface, and bind immunoglobulins. The two AAV2-Z34C mutants (wt587Z34C and wt587Δ9Z34C) were analyzed for their ability to package the viral genome. Each mutant could be efficiently packaged (Table 1). When analyzed by electron microscopy, both mutants showed a normal capsid morphology. However, two to three times more empty particles were detected with the mutants than with wild-type AAV2 (Fig. 2 and Table 1). To determine whether the

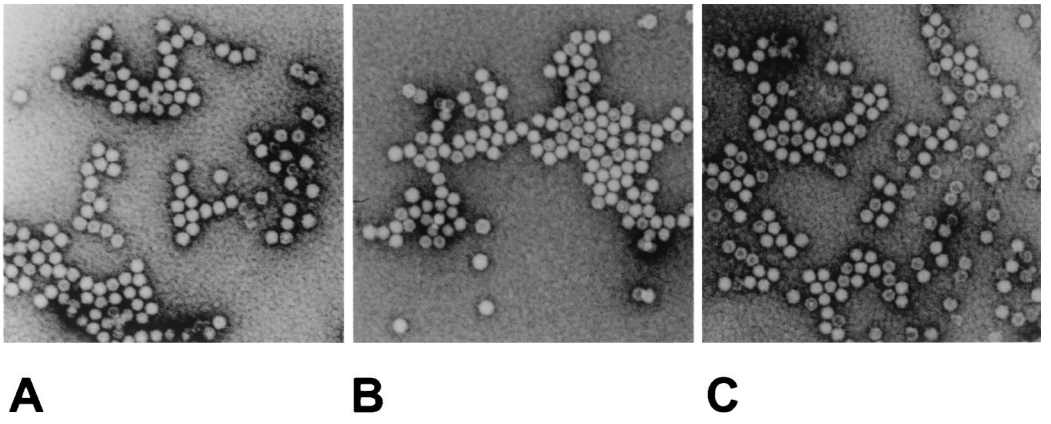

FIG. 2. Electron microscopy analysis of AAV2 and AAV2-Z34C mutants. (A) Wild-type AAV2. (B) wt587Z34C. (C) wt587Δ9Z34C. Empty capsids can be recognized as viral capsids with black centers. Titers were calculated in comparison to a known viral standard.

structures of wt587Z34C and wt587Δ9Z34C were similar to that of wild-type AAV2, we performed an ELISA with MAB A20, which specifically reacts with completely assembled AAV2 capsids and allows the calculation of wild-type analog AAV2 particles (28). A20 reacted with both mutants. Capsid titers of $>10^{11}$ particles/ml were achieved, a value which represented only a 5- to 11-fold reduction in the EM:A20$^+$ titer ratio compared to that for wild-type AAV2 (Table 1). Because the binding of the murine IgG1 constant region of A20 to Z34C is orders of magnitude less efficient than A20 variable region binding to specific viral surface epitopes, a disturbance of the A20-positive titer determination could be excluded (data not shown). In Western blot analysis, the distribution of VP1, VP2, and VP3 proteins in viral capsids was identical to that in wild-type AAV2, i.e., 1:1:10 (data not shown).

The infectivity of AAV2-Z34C mutants for HeLa cells, which were used as indicator cells for natural tropism, was reduced from 5×10^9 Rep EFU/ml (wild-type AAV2) to 3×10^5 Rep EFU/ml (wt587Z34C) and 1×10^6 Rep EFU/ml (wt587Δ9Z34C). Analogous results were achieved with recombinant vectors and with GFP as a transgene (Table 1).

Next, we wished to determine whether Z34C was expressed on the capsid surface and whether it was functional. Using an ELISA, wild-type AAV2 or AAV2-Z34C particles were directly attached to microtiter plates, and the binding of biotinylated antibodies from different species (human, rabbit, and mouse) was measured. With both mutants, specific immunoglobulin binding was observed, whereas wild-type AAV2 showed only weak, nonspecific binding. Figure 3 shows the binding of rabbit IgG in a representative experiment. The optical density was elevated at least three- to fivefold compared to that of the controls. Mutant wt587Z34C reacted considerably stronger with antibodies than wt587Δ9Z34C, suggesting that the combination of a 9-aa deletion with the insertion of Z34C was not advantageous in terms of immunoglobulin binding. Antibodies from other species (human and mouse IgG2a-IgG2b and rabbit IgG) bound with comparable affinities to both AAV2-Z34C mutants. The same differences in binding affinities were observed for the two mutants (data not shown).

Retargeting of rAAV to distinct hematopoietic cells. To evaluate the retargeting of the rAAV-Z34C mutants, the hematopoietic cell lines M-07e (acute myeloid leukemia with megakaryocytic differentiation; M7) (1), Jurkat (T-cell leukemia), and Mec1 (chronic lymphatic leukemia; B-CLL) (24) were selected, because previous work had demonstrated that a specific and/or efficient transduction of these cells by AAV2-derived vectors was difficult (Table 2) (2). The transduction of target cells with unmutated rAAV-GFP vectors yielded titers of 2×10^4 to 2×10^5 GFP EFU/ml (Table 2).

The hematopoietic cell surface receptors CD29 (β_1-integrin), CD117 (c-kit stem cell factor receptor), and CXCR4 (coreceptor of human immunodeficiency virus) were chosen as potential targeting receptors. For this purpose, we used a mouse anti-CD29 MAb (IgG2a; Immunotec), a rabbit poly-

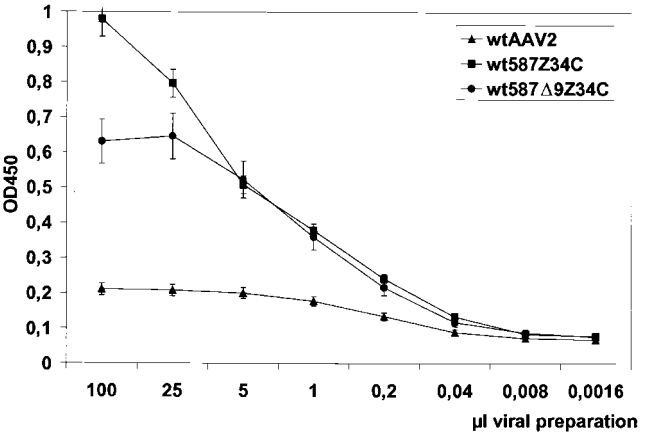

FIG. 3. Presentation and functionality of the Z34C ligand on AAV2 mutants. An ELISA was used to detect the Z34C ligand and its immunoglobulin binding affinity. The binding of rabbit IgG1 to wt587Z34C, wt587Δ9Z34C, and wild-type AAV2 (wtAAV2) is shown. Serial dilutions of viral preparations were used to coat 96-well plates overnight at 4°C and were blocked with PBS containing 2% BSA and 0.05% Tween. After a wash with PBS, biotinylated rabbit antibody was added (2.5 μg/ml in PBS), and the plates were incubated at room temperature for 1 h. Detection of Z34C-bound biotinylated antibody was performed as described in Material and Methods. Virus volumes are shown as titers in Table 1. OD450, optical density at 450 nm. Error bars show standard deviations.

TABLE 2. Retargeting to M-07e, Jurkat, and Mec1 cells by recombinant Z34C mutants and antibodies against CD29, CD117, and CXCR4[a]

Cells	Antibodies	Virus	Titer (GFP EFU/ml) under the following conditions[b]:				
			−/−/−/	+/−/−/	+/+/−/	−/+/−/	−/−/+/
M-07e	CD117	rAAV-GFP	2×10^5	2×10^5	2×10^5	2×10^5	9×10^2
		rAAV-GFP587Z34C	<1	2×10^3	2×10^3	<1	<1
		rAAV-GFP587Δ9Z34C	<1	<1	ND	ND	ND
Jurkat	CD29	rAAV-GFP	2×10^4	2×10^4	2×10^4	2×10^4	<1
		rAAV-GFP587Z34C	<1	1×10^3	1×10^3	<1	<1
		rAAV-GFP587Δ9Z34C	<1	<1	ND	ND	ND
Jurkat	CXCR4	rAAV-GFP	2×10^4	2×10^4	2×10^4	2×10^4	<1
		rAAV-GFP587Z34C	<1	1×10^3	1×10^3	<1	<1
		rAAV-GFP587Δ9Z34C	<1	<1	ND	ND	ND
Mec1	CD29	rAAV-GFP	2×10^5	2×10^5	2×10^5	2×10^5	1×10^2
		rAAV-GFP587Z34C	<1	2×10^3	2×10^3	<1	<1
		rAAV-GFP587Δ9Z34C	<1	<1	ND	ND	ND
Mec1	CXCR4	rAAV-GFP	2×10^5	2×10^5	2×10^5	2×10^5	1×10^2
		rAAV-GFP587Z34C	<1	3×10^3	3×10^3	<1	<1
		rAAV-GFP587Δ9Z34C	<1	<1	ND	ND	ND
HeLa	—[c]	rAAV-GFP	5×10^7	5×10^7	5×10^7	5×10^7	8×10^2
		rAAV-GFP587Z34C	2×10^4	5×10^3	2×10^4	2×10^4	<1
		rAAV-GFP587Δ9Z34C	2×10^4	1×10^3	2×10^4	2×10^4	<1

[a] Control experiments were done with HeLa cells.
[b] Infections were done with (+) or without (−) targeting antibody/inhibitory protein A (10 μg/ml) or IgG (2 μg/ml)/AAV tropism-blocking heparin (100 μg/ml). No inhibition of transduction by the retargeting vectors was obtained with heparin. Inhibitory protein A or IgG was used independently and provided the same results. ND, not done.
[c] —, identical results were obtained with anti-CD29, anti-CXCR4, and anti-CD117 antibodies.

clonal anti-CD117 antiserum (ImoGenex), and a rabbit polyclonal anti-CXCR4 antiserum (N terminus specific; Chemicon). The expression of these target receptors on the surface of the target cell lines and the binding of the specific antibodies were confirmed by fluorescence-activated cell sorting analysis prior to testing in retargeting experiments (data not shown). All three receptors are known to mediate the uptake of their bound ligands and have already been used successfully for retargeting of other viruses (13, 32).

For transduction of hematopoietic cells, rAAV2-Z34C vectors (with GFP as a transgene) were loaded with the specific targeting antibodies and incubated for 24 h with irradiated target cells. Cells were analyzed for GFP gene expression 48 h after infection by fluorescence microscopy and flow cytometry. Specific retargeting was detected with mutant rAAV-GFP587Z34C on M-07e, Jurkat, and Mec1 cells. Different combinations of cells and antibodies against CD29, CD117, and CXCR4 were used to correspond to the different expression of these receptors on the different cell types, as shown in Table 2. Titers were estimated to be as high as 1×10^3 to 3×10^3 GFP EFU/ml. No retargeting or infection could be observed when the virus mutant was used without antibody (<1 GFP EFU/ml). rAAV2-Z34C transduction was specifically antibody mediated, because it could be blocked with soluble protein A or IgG molecules but not with heparin, which was used to block the natural receptor binding site of AAV2 (27).

Performing infection experiments by binding of virus-antibody complexes and inhibitory molecules at 4°C, washing, and shifting to 37°C did not affect or enhance transduction efficiency. In control experiments, antibodies against the targeted receptors did not enhance the infectivity of unmutated AAV2 vectors themselves (data not shown). No retargeting could be detected with mutant rAAV-GFP587Δ9Z34C. In addition, no retargeting was detected with antibodies against CD20, CD21, and HLA molecules. Infection of HeLa cells by AAV-Z34C mutants was reduced when the virus was loaded with any of the antibodies against targeting receptors not expressed on HeLa cells.

As an example, the retargeting and transduction of the B-CLL cell line Mec1 by the rAAV-GFP587Z34C vector conjugated to the anti-CXCR4 antibody are shown in Fig. 4. No transduction could be observed without the antibody (Fig. 4A), whereas the addition of the anti-CXCR4 antibody mediated specific, heparin-independent transduction of the cells (Fig. 4B).

DISCUSSION

This report presents a new AAV targeting strategy using a minimized domain of protein A and various antibodies binding to specific cell surface receptors. By insertion of an immunoglobulin binding domain into the capsid of AAV2, monoclonal or polyclonal antibodies were bound and allowed rAAV2 vectors expressing the GFP marker gene to be retargeted to specific hematopoietic cells.

The insertion size at AAV2 capsid position 578 is strictly limited (unpublished data). Therefore, we had to insert a relatively small coupling peptide into the AAV2 capsid. One possibility was the use of immunoglobulin binding proteins recognizing the Fc domain, since this would leave the variable

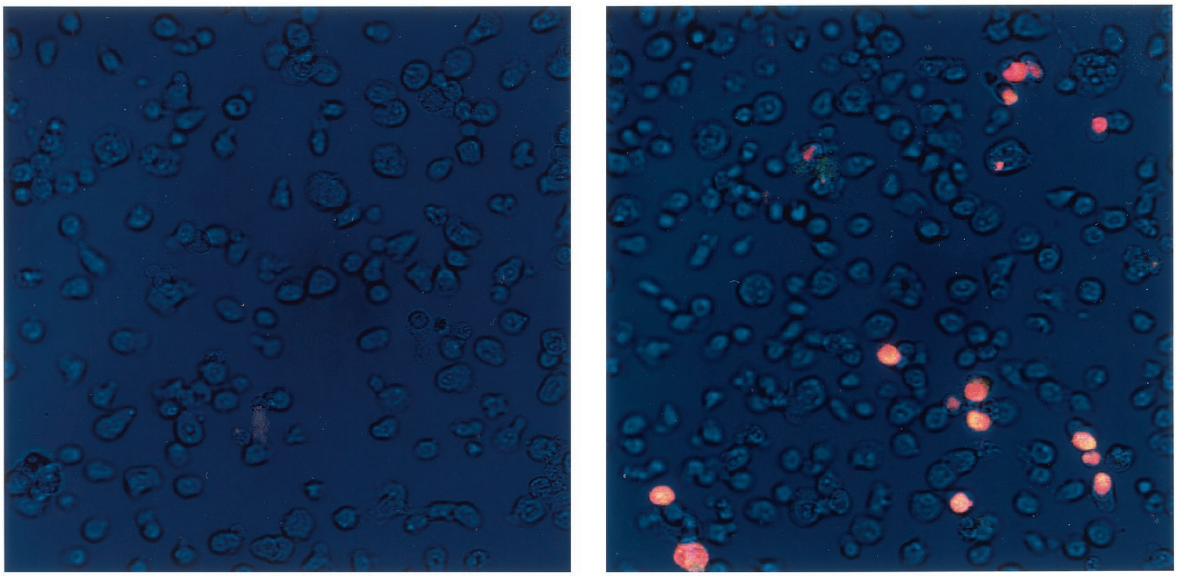

FIG. 4. Transduction of Mec1 cells. Infection of Mec1 cells by rAAV-GFP587Z34C without (A) or with (B) anti-CXCR4 antibody was examined. Light microscopy was done with a confocal integrated GFP immunofluorescence overlay of infected cells.

domain of the immunoglobulin free for interacting with the specific cellular epitopes. Fortunately, a minimized binding motif of *S. aureus* protein A, Z34C, was described recently (25). Although the optimized Z34C domain of protein A shows a higher exchange rate, the binding affinity is reduced only twofold in comparison to that of the natural B domain. A large dimer of the Z domain of protein A was already used successfully for the retargeting of Sindbis virus (15, 16). The insertion of the Z34C ligand at position 587 resulted in a relatively modest reduction in packaging efficiency in comparison to that of the wild-type capsid (Table 1). The reduced packaging efficiency of the AAV2-Z34C mutants was explained at least in part by the generation of more empty capsids than were observed with the wild-type AAV2 capsid. This packaging efficiency also seemed to be affected by the size of the inserted ligand, because the combination of the insertion with a 9-aa deletion allowed packaging efficiency comparable to that of wild-type AAV2 to be maintained. Fortunately, the ligand insertion at position 587 did not affect the capsid morphology, as shown by electron microscopy and an ELISA specific for fully assembled capsids. Reduced packaging efficiency of mutants in combination with a transgene (GFP) was often observed with position 587 mutants (unpublished data). A hypothetical explanation of this observation is that the capsid stability of the position 587 mutants may be decreased.

Infection of HeLa cells, which was used to indicate the natural tropism of AAV2, was reduced up to 4 orders of magnitude. The explanation for this reduced infection via the wild-type AAV2 receptor is most likely disruption of the natural receptor binding site by the ligand insertion at position 587 (29). In heparin binding experiments, the affinity for heparin columns is reduced with all position 587 mutants (data not shown). However, in order to fully eliminate the natural host tropism, additional modifications of the viral capsid may be necessary. Infectivity for HeLa cells was reduced when Z34C mutants were loaded with targeting antibodies whose receptors were not expressed on HeLa cells. Epitopes on the viral capsid essential for natural receptor interactions probably were covered by the bound antibodies.

The insertion of Z34C at position 587 allowed functional expression of the immunoglobulin binding domain on the capsid surface. Both mutants wt587Z34C and wt587Δ9Z34C showed significant immunoglobulin binding. When added at comparable titers, wt587Z34C showed more effective antibody binding than wt587Δ9Z34C. Most likely, the reduced efficiency of antibody binding explained the failure of mutant wt587Δ9Z34C to transduce cells specifically.

The infection was specifically antibody mediated. No transduction could be detected with mutant rAAV2-GFP587Z34C without antibody, whereas the targeted infection could be blocked with soluble protein A or IgG molecules. In addition, no inhibition of transduction by the retargeting vectors was obtained with heparin, which blocks the natural receptor binding site of AAV2 (27). This result demonstrated that the interaction of the AAV2-Z34C mutants with the natural AAV receptor was not essential for infection or transduction and proved the altered infection profile and independence for HSPG (retargeting) (30). Although the transduction efficiency was reduced in comparison to that of the wild-type AAV2 capsid, the specificity of transduction was highly increased and could be targeted to specific receptors expressed on hematopoietic cells. This study provides the first demonstration that rAAV vectors can be targeted to specific cell receptors by use of a universal targeting approach.

Until now, targeting of viral vectors to hematopoietic cells has been tried by using retroviruses with short ligands or an-

tibody single-chain fragments inserted into the virus envelope (21). Engelstädter et al., who transduced Jurkat cells with a retrovirus targeted with antibody domains from a phage display library (5), achieved titers of up to 3×10^5 EFU/ml. The protein A targeting strategy used by Ohno et al. with the Z domain and Sindbis virus resulted in infectious titers of up to 2×10^5 infectious particles per ml with antibodies against CD4-positive cells (15, 16).

Different strategies were used in two recent studies to retarget AAV2 to hematopoietic cells. Yang et al. added the single-chain fragment variable region of an anti-CD34 MAb to the N terminus of the VP2 capsid protein (33). Although they obtained retargeted AAV2 virions, they achieved only low titers of up to 4×10^2 infectious virions per ml. A single-chain fragment variable region–VP2 fusion protein was used. Nonmutated capsid proteins were needed for virus assembly. This procedure made the composition of the viral capsid unpredictable. Another approach to retargeting of AAV2 is the use of bispecific antibodies recognizing the AAV2 capsid (through one Fab arm) and the alternative target cell surface receptor (through the other Fab arm) (2). This strategy allowed the transduction of the megakaryocytic leukemia cell line M-07e via the vector-bispecific antibody complex. However, it remains difficult and time-consuming to establish new bispecific antibodies for each cell type and targeting approach.

Recently, several groups tried to characterize the AAV2 capsid by random insertional mutagenesis or antibody epitope mapping (14, 19, 20, 30). Although these studies provided important insights into potential receptor binding sites and confirmed the relevance of position 587 as a virus receptor binding site (6, 29), no cell-type-specific retargeting was achieved. The results of this study may be a first step toward specific retargeting of rAAV2 to hematopoietic cells. Another practical application of this system may be the ability to rapidly and efficiently purify the rAAV587Z34C capsid on an affinity column. The insertion of immunoglobulin binding domains into the AAV2 capsid may provide a fast and universal targeting strategy for AAV2 vectors, in particular, for ex vivo gene transfer into hematopoietic cells. With these vectors, it may be possible to transduce specific hematopoietic cells. In addition, we will test different strategies for covalent coupling of antibodies to the viral capsid in order to use this system for an in vivo approach in the future. In addition, we will characterize the uptake mechanism for these specific targeting constructs by single virus tracing (23).

Taken together, this study provides the first demonstration that rAAV vectors can be targeted to specific cell surface receptors by use of a universal targeting approach with immunoglobulin binding domains. Given this proof of principle, our group is currently testing additional capsid mutants and immunoglobulin binding domains in order to combine high targeting specificity with higher transduction efficiency.

ACKNOWLEDGMENTS

We are grateful to Jürgen Kleinschmidt and Christiane Wobus (DKFZ) for providing AAV-specific antibodies and performing electron microscopy of AAV mutants.

This work was supported by a grant from the Deutsche Forschungsgemeinschaft (SFB 455) (to M.H.) and by stipends from the Studienstiftung des Deutschen Volkes and the Fond der Chemischen Industrie (BMBF) (to M.U.R.)

REFERENCES

1. **Avanzi, G. C., M. F. Brizzi, J. Giannotti, A. Ciarletta, Y. C. Yang, L. Pegoraro, and S. C. Clark.** 1990. M-07e human leukemic factor-dependent cell line provides a rapid and sensitive bioassay for the human cytokines GM-CSF and IL-3. J. Cell Physiol. **145:**458–464.
2. **Bartlett, J. S., J. Kleinschmidt, R. C. Boucher, and R. J. Samulski.** 1999. Targeted adeno-associated virus vector transduction of nonpermissive cells mediated by a bispecific $F(ab'\gamma)_2$ antibody. Nat. Biotechnol. **17:**181–186.
3. **Chiorini, J. A., C. M. Wendtner, E. Urcelay, B. Safer, M. Hallek, and R. M. Kotin.** 1995. High-efficiency transfer of the T cell co-stimulatory molecule B7–2 to lymphoid cells using high-titer recombinant adeno-associated virus vectors. Hum. Gene Ther. **6:**1531–1541.
4. **Conway, J. E., C. M. Rhys, I. Zolotukhin, S. Zolotukhin, N. Muzyczka, G. S. Hayward, and B. J. Byrne.** 1999. High-titer recombinant adeno-associated virus production utilizing a recombinant herpes simplex virus type I vector expressing AAV-2 Rep and Cap. Gene Ther. **6:**986–993.
5. **Engelstädter, M., M. Bobkova, M. Baier, J. Stitz, N. Holtkamp, T. H. Chu, R. Kurth, R. Dornburg, C. J. Buchholz, and K. Cichutek.** 2000. Targeting human T cells by retroviral vectors displaying antibody domains selected from a phage display library. Hum. Gene Ther. **11:**293–303.
6. **Girod, A., M. Ried, C. Wobus, H. Lahm, K. Leike, J. Kleinschmidt, G. Deleage, and M. Hallek.** 1999. Genetic capsid modifications allow efficient re-targeting of adeno-associated virus type 2. Nat. Med. **5:**1052–1056.
7. **Grimm, D., A. Kern, M. Pawlita, F. Ferrari, R. Samulski, and J. Kleinschmidt.** 1999. Titration of AAV-2 particles via a novel capsid ELISA: packaging of genomes can limit production of recombinant AAV-2. Gene Ther. **6:**1322–1330.
8. **Hacker, U. T., F. M. Gerner, H. Buning, M. Hutter, H. Reichenspurner, M. Stangl, and M. Hallek.** 2001. Standard heparin, low molecular weight heparin, low molecular weight heparinoid, and recombinant hirudin differ in their ability to inhibit transduction by recombinant adeno-associated virus type 2 vectors. Gene Ther. **8:**966–968.
9. **Hallek, M., and C. M. Wendtner.** 1996. Recombinant adeno-associated virus (rAAV) vectors for somatic gene therapy: recent advances and potential clinical applications. Cytokines Mol. Ther. **2:**69–79.
10. **Handa, A., S. Muramatsu, J. Qiu, H. Mizukami, and K. E. Brown.** 2000. Adeno-associated virus (AAV)-3-based vectors transduce haematopoietic cells not susceptible to transduction with AAV-2-based vectors. J. Gen. Virol. **81:**2077–2084.
11. **Kotin, R. M.** 1994. Prospects for the use of adeno-associated virus as a vector for human gene therapy. Hum. Gene Ther. **5:**793–801.
12. **Laughlin, C. A., J. D. Tratschin, H. Coon, and B. J. Carter.** 1983. Cloning of infectious adeno-associated virus genomes in bacterial plasmids. Gene **23:** 65–73.
13. **Mebatsion, T., S. Finke, F. Weiland, and K. K. Conzelmann.** 1997. A CXCR4/CD4 pseudotype rhabdovirus that selectively infects HIV-1 envelope protein-expressing cells. Cell **90:**841–847.
14. **Moskalenko, M., L. Chen, M. van Roey, B. A. Donahue, R. O. Snyder, J. G. McArthur, and S. D. Patel.** 2000. Epitope mapping of human anti-adeno-associated virus type 2 neutralizing antibodies: implications for gene therapy and virus structure. J. Virol. **74:**1761–1766.
15. **Ohno, K., and D. Meruelo.** 1997. Retrovirus vectors displaying the IgG-binding domain of protein A. Biochem. Mol. Med. **62:**123–127.
16. **Ohno, K., K. Sawai, Y. Iijima, B. Levin, and D. Meruelo.** 1997. Cell-specific targeting of Sindbis virus vectors displaying IgG-binding domains of protein A. Nat. Biotechnol. **15:**763–767.
17. **Ponnazhagan, S., P. Mukherjee, X. S. Wang, K. Qing, D. M. Kube, C. Mah, C. Kurpad, M. C. Yoder, E. F. Srour, and A. Srivastava.** 1997. Adeno-associated virus type 2-mediated transduction in primary human bone marrow-derived $CD34^+$ hematopoietic progenitor cells: donor variation and correlation of transgene expression with cellular differentiation. J. Virol. **71:**8262–8267.
18. **Qing, K., C. Mah, J. Hansen, S. Zhou, V. Dwarki, and A. Srivastava.** 1999. Human fibroblast growth factor receptor 1 is a co-receptor for infection by adeno-associated virus 2. Nat. Med. **5:**71–77.
19. **Rabinowitz, J. E., and R. J. Samulski.** 2000. Building a better vector: the manipulation of AAV virions. Virology **278:**301–308.
20. **Rabinowitz, J. E., W. Xiao, and R. J. Samulski.** 1999. Insertional mutagenesis of AAV2 capsid and the production of recombinant virus. Virology **265:**274–285.
21. **Russell, S. J., and F. L. Cosset.** 1999. Modifying the host range properties of retroviral vectors. J. Gene Med. **1:**300–311.
22. **Samulski, R. J., L. S. Chang, and T. Shenk.** 1987. A recombinant plasmid from which an infectious adeno-associated virus genome can be excised in vitro and its use to study viral replication. J. Virol. **61:**3096–3101.
23. **Seisenberger, G., M. U. Ried, T. Endress, H. Buning, M. Hallek, and C. Brauchle.** 2001. Real-time single-molecule imaging of the infection pathway of an adeno-associated virus. Science **294:**1929–1932.
24. **Stacchini, A., M. Aragno, A. Vallario, A. Alfarano, P. Circosta, D. Gottardi, A. Faldella, G. Rege-Cambrin, U. Thunberg, K. Nilsson, and F. Caligaris-Cappio.** 1999. MEC1 and MEC2: two new cell lines derived from B-chronic

lymphocytic leukaemia in prolymphocytoid transformation. Leuk. Res. **23:** 127–136.
25. **Starovasnik, M. A., A. C. Braisted, and J. A. Wells.** 1997. Structural mimicry of a native protein by a minimized binding domain. Proc. Natl. Acad. Sci. USA **94:**10080–10085.
26. **Summerford, C., J. S. Bartlett, and R. J. Samulski.** 1999. AlphaVbeta5 integrin: a co-receptor for adeno-associated virus type 2 infection. Nat. Med. **5:**78–82.
27. **Summerford, C., and R. J. Samulski.** 1998. Membrane-associated heparan sulfate proteoglycan is a receptor for adeno-associated virus type 2 virions. J. Virol. **72:**1438–1445.
28. **Wistuba, A., A. Kern, S. Weger, D. Grimm, and J. A. Kleinschmidt.** 1997. Subcellular compartmentalization of adeno-associated virus type 2 assembly. J. Virol. **71:**1341–1352.
29. **Wobus, C. E., B. Hugle-Dorr, A. Girod, G. Petersen, M. Hallek, and J. A. Kleinschmidt.** 2000. Monoclonal antibodies against the adeno-associated virus type 2 (AAV-2) capsid: epitope mapping and identification of capsid domains involved in AAV-2–cell interaction and neutralization of AAV-2 infection. J. Virol. **74:**9281–9293.
30. **Wu, P., W. Xiao, T. Conlon, J. Hughes, M. Agbandje-McKenna, T. Ferkol, T. Flotte, and N. Muzyczka.** 2000. Mutational analysis of the adeno-associated virus type 2 (AAV2) capsid gene and construction of AAV2 vectors with altered tropism. J. Virol. **74:**8635–8647.
31. **Xiao, X., J. Li, and R. J. Samulski.** 1998. Production of high-titer recombinant adeno-associated virus vectors in the absence of helper adenovirus. J. Virol. **72:**2224–2232.
32. **Yajima, T., T. Kanda, K. Yoshiike, and Y. Kitamura.** 1998. Retroviral vector targeting human cells via c-Kit–stem cell factor interaction. Hum. Gene Ther. **9:**779–787.
33. **Yang, Q., M. Mamounas, G. Yu, S. Kennedy, B. Leaker, J. Merson, F. Wong-Staal, M. Yu, and J. R. Barber.** 1998. Development of novel cell surface CD34-targeted recombinant adenoassociated virus vectors for gene therapy. Hum. Gene Ther. **9:**1929–1937.
34. **Zolotukhin, S., B. J. Byrne, E. Mason, I. Zolotukhin, M. Potter, K. Chesnut, C. Summerford, R. J. Samulski, and N. Muzyczka.** 1999. Recombinant adeno-associated virus purification using novel methods improves infectious titer and yield. Gene Ther. **6:**973–985.